Exploring the Distant Universe With the Spitzer Space Telescope

Sarah J. U. Higdon*, James L. Higdon*, Dan Weedman*, James R. Houck*, B. T. Soifer†, Lee Armus†, Vassilis Charmandaris* and Terry L. Herter*

*Astronomy Dept., Cornell University, Ithaca, NY 14853
†Spitzer Science Center, MC 220-6, California Institute of Technology, Pasadena, CA 91125

Abstract.
The infrared Spitzer Space Telescope is the last of NASA's Great Observatories. Highlights of the first results from the Infrared Spectrograph (IRS) Extragalactic Team are given. The main focus of this paper is a demonstration of the unprecedented sensitivity of the IRS, which makes observations of distant, dust enshrouded galaxies possible.

INTRODUCTION

The Spitzer Space Telescope (SST) is the final cornerstone in the NASA Great Observatory program, which includes the Hubble Space Telescope, the Chandra X-ray Observatory and the Compton Gamma Ray Observatory. Figure 1 shows the launch of SST from Cape Canaveral, Florida on 2003 August 25. Unlike the other Great Observatories, SST is in an Earth-trailing solar orbit, drifting away from the Earth at the rate of $\sim$ 15 million kilometers (0.1 AU) per year. SST's primary mirror is 85cm in diameter. It is a cryogenically-cooled infrared telescope and was launched with 360 liters of liquid helium. The predicted cryogenic lifetime is $\sim$ 5 yrs. Further observatory details are given in [1].

SST has three instruments, two cameras and a spectrograph. The Infrared Spectrograph (IRS) [2] comprises four separate modules covering the wavelength range from 5.3 to 38 μm with spectral resolutions, R = $\lambda/\Delta\lambda \sim$ 90 and 600. Figure 2 shows the IRS. The modules are named after their wavelength coverage and resolution as Short-Low (SL), Short-High (SH), Long-Low (LL) and Long-High (LH). The SL module includes two peak-up imaging cameras. Both the "blue" (centered at 16 μm) and "red" (centered at 22 μm) cameras have a $\sim$ 1 sq. arcmin field of view (FOV). The IRS is optimized for sensitivity as demonstrated in Section 3. The remaining two instruments are designed for large area surveys. The Infrared Array Camera (IRAC) [3] has four channels that obtain simultaneous broadband images. The channels are paired so that data is obtained at at 3.6 & 5.8 μm in one 5.2 square arcmin FOV and simultaneously at 4.5 & 8.0 μm in a separate 5.2 square arcmin FOV. The Multiband Imaging Photometer for Spitzer (MIPS) [4] is capable of imaging in three broad spectral bands centered at 24, 70, and 160 microns, each with a $\sim$ 5 arcmin square FOV, a 2.5 arcmin by 5 arcmin FOV and a 0.5 arcmin by 5 arcmin FOV, respectively. MIPS can also take low-resolution (R = $\lambda/\Delta\lambda \sim$ 15) spectra between 51 and 106 μm. For further details of the three SST instruments see the Spitzer Observers Manual [1]

SST can observe a wide range of objects both nearby (e.g. in our Solar System) and far (e.g. The IRS has observed a z = 6.4 quasar). In this paper we will highlight some of the first results from the IRS Guaranteed Time Extragalactic program. Throughout this paper we adopt a flat Λ-dominated universe with $H_0 = 71$ kms^{-1} Mpc^{-1}, $\Omega_M = 0.27$ and $\Omega_0 = 0.73$.

[1] http://ssc.spitzer.caltech.edu/documents/som/

CP743, *The New Cosmology: Conference on Strings and Cosmology and The Mitchell Symposium on Observational Cosmology*
edited by R. E. Allen, D. V. Nanopoulos, and C. N. Pope

FIGURE 1. The Spitzer Space Telescope is launched into space aboard a Boeing Delta II Heavy rocket (Delta 7920H ELV) in the early morning hours of August 25, 2003, from Cape Canaveral Air Force Station in Florida. Photo Credit: NASA/JPL-Caltech

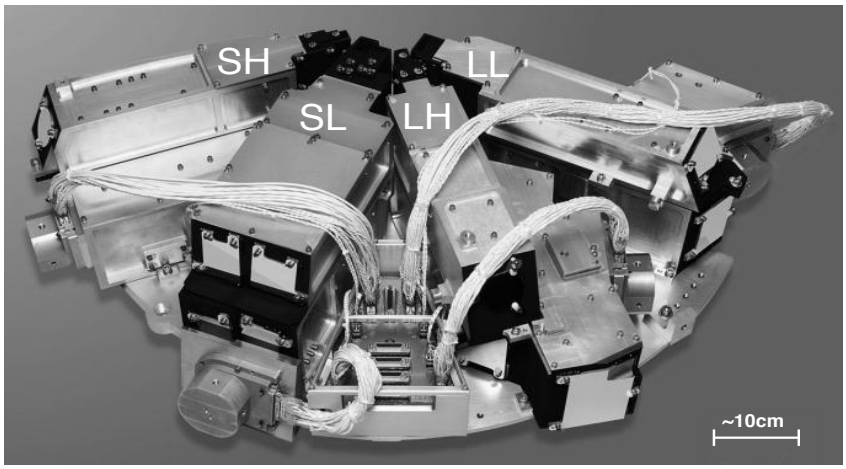

FIGURE 2. The IRS, photo credit: Ball Aerospace

ULTRALUMINOUS INFRARED GALAXIES

We are conducting a large survey of Ultraluminous Infrared Galaxies (ULIRGs) with the Infrared Spectrograph on the Spitzer Space Telescope, which will result in low (R $\sim$ 90) and high (R $\sim$ 600) spectral resolution spectra from 5 to 38.5 μm of 110 sources with redshifts of $0.02 < z < 0.90$. ULIRGs have the power output of quasars yet emit nearly all of their energy in the infrared, with $L_{IR} \geq 10^{12}\ L_{\odot}$. The majority of ULIRGs are found in interacting and merging systems (e.g., Armus et al. [5]; Sanders et al. [6] & Murphy et al. [7]). During the merger process large quantities of molecular and atomic gas and dust are driven toward the nucleus (or nuclei) fueling a massive starburst and/or active galactic nucleus (AGN [8]). Although rare in the local Universe, it is thought that ULIRGs make a significant contribution to both the star-formation energy density and the far-infrared background (e.g., Blain et al. [9]) at high redshifts, i.e. $z \geq 2$.

We presented our first results in Armus et al. [10]. Three nearby ULIRGs were selected from our sample which

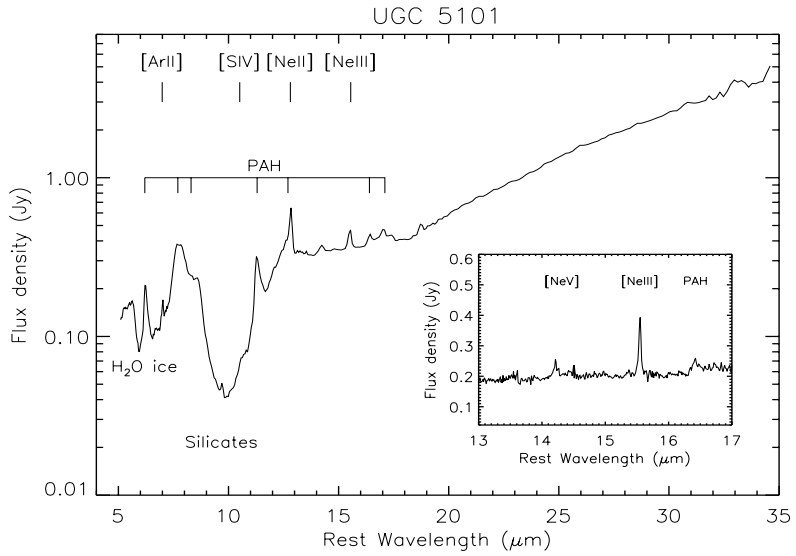

FIGURE 3. IRS Short-Low and Long-Low spectra of the ULIRG UGC 5101. Prominent emission lines and absorption bands (the latter indicated by horizontal bars) are marked. Open diamonds are the IRAS 12 and 25 μm points. Inset is the high resolution observation of [NeV] 14.32 μm , [NeIII] 15.56 μm & PAH 16.4 μm.

display a wide range of spectral properties and the results are summarized here. UGC 5101 (z = 0.039) has a disturbed morphology suggestive of a merger [6]. Optically, UGC 5101 is classified as a LINER [11]. The IRAS 25 μm / IRAS 60 μm flux ratio is $\sim$ 0.1 and UGC 5101 is classified as a cold, starburst-dominated, far-infrared source. ISO SWS and PHT-S spectroscopy [12] also indicate a powerful, circumnuclear starburst. However, XMM-Newton data found an obscured, but luminous, hard X-ray source with $L_{2-10keV} \sim 5 \times 10^{42}$ ergs s^{-1} and $L_{2-10keV}/L_{IR} \sim 0.002$ suggestive of a heavily obscured AGN [13]. As seen in Figure 3, we detect the [Ne V] 14.3 μm emission line, providing the first direct evidence for a buried AGN in the mid-infrared (MIR).

Mrk 463 (z = 0.0508) is a merging system with two nuclei separated by about 4$''$ (Mrk 463E & Mrk 463W, [14]). Both nuclei have Seyfert 2 optical spectra [15], but broad lines are seen in scattered optical [16] and direct near-infrared light [17, 18]. Although the far-infrared luminosity of Mrk 463 (5×10^{11} L$_\odot$) is slightly less than the canonical ULIRG cutoff of 10^{12} L$_\odot$, the bolometric luminosity of this system is very high, and it was included in the first results paper.

Mrk 1014 (z = 0.1631) is a radio-quiet, infrared luminous QSO with broad optical emission lines (FWHM H$_\beta$ > 4000 km s^{-1}) and twin tidal tails indicative of a recent interaction and merger [19]. Both Mrk 463 and Mrk 1014 are classified as warm AGN dominated far-infrared sources with IRAS 25 μm / IRAS 60 μm flux ratios greater than 0.2 (0.74 and 0.27, respectively [20]).

It can be seen in Figures 3 & 4 that both UGC 5101 and Mrk 463 show strong silicate absorption suggesting large optical depths to the nuclei at 10 μm. UGC 5101 also shows the clear presence of water ice in absorption. Polycyclic aromatic hydrocarbon (PAH) emission features are seen in both Mrk 1014 and UGC 5101. We also detect the 16.4 μm PAH feature (e.g., Moutou et al. [21]) in UGC 5101. To our knowledge, this is the first detection of this feature in a ULIRG, although it is seen in some nearby starburst galaxies [22, 23]. The fine-structure lines are consistent with dominant AGN power sources in both Mrk 1014 and Mrk 463. For example, the [Ne V] 14.32/[Ne II] 12.81 line flux ratio in Mrk 1014 suggests that nearly all the ionizing flux (> 80 - 90 % based on the simple scaling models in Sturm et al. [24]) comes from the AGN.

total

These first observations show a diverse range in spectral features. To date we have observed $\sim$ 70 ULIRGs. The results from the analysis of this large sample will be a set of powerful diagnostics that can be used to understand the nature of obscured galaxies at even higher redshift (z $\geq$2).

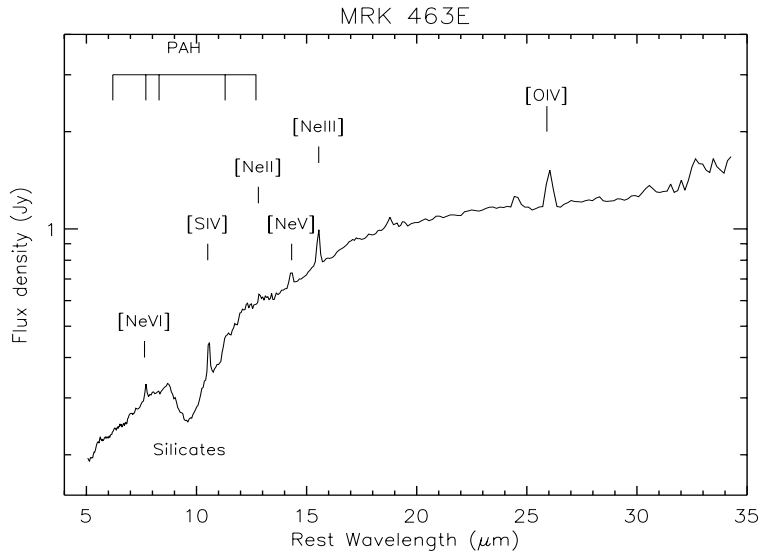

FIGURE 4. IRS Short-Low and Long-Low spectra of the ULIRG Mrk 463e. Prominent emission lines and absorption bands (the latter indicated by horizontal bars) are marked. Open diamonds are the IRAS 12 and 25 μm points.

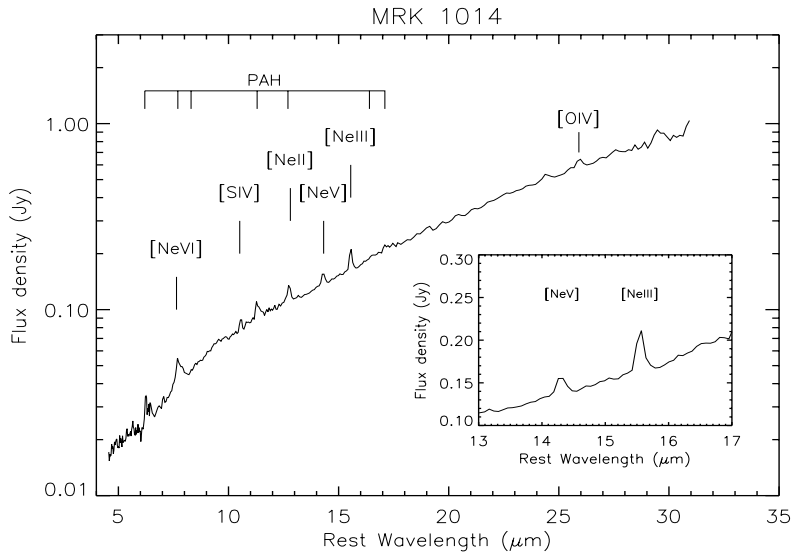

FIGURE 5. IRS Short-Low and Long-Low spectra of the ULIRG Mrk 1014. Prominent emission lines and absorption bands (the latter indicated by horizontal bars) are marked. Open diamonds are the IRAS 12 and 25 μm points. Inset is the high resolution observation of the [NeV] 14.32 μm & [NeIII] 15.56 μm lines

FIRST MID-IR SPECTRUM OF A FAINT HIGH-Z GALAXY

Many important discoveries from SST will derive from wide area surveys, which are revealing large numbers of infrared galaxies. The unprecedented sensitivity of the IRS allows for the first time the measurement of mid-infrared spectra from 14 μm to 38 μm of faint high-z galaxies. Such spectra are crucial in characterizing the nature of newly discovered distant galaxies, which are too faint for optical follow-up. We demonstrated this unique capability with an

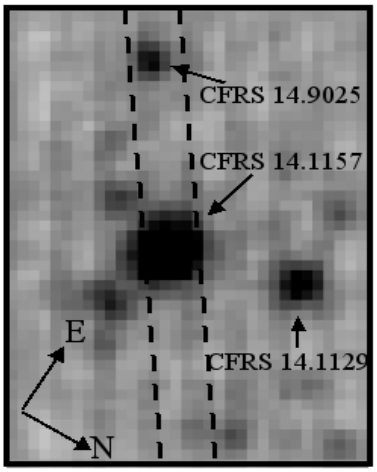

FIGURE 6. Image from the Blue Peak up Camera on the IRS, having field of view 60" by 72" and integration time 48 seconds. Dashed line is the LL slit position generated by the Spitzer Planning Observations Tool (SPOT).

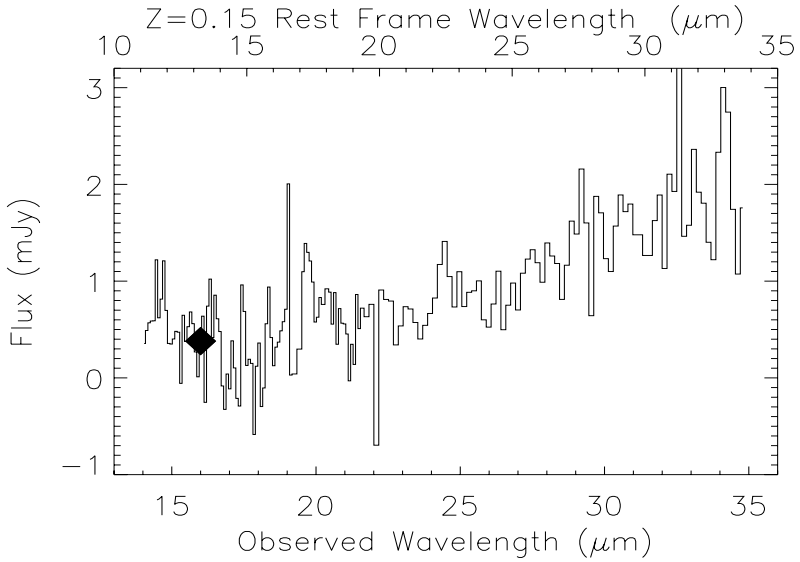

FIGURE 7. IRS-LL spectrum of CFRS 14.9025 (z = 0.155) obtained after 1440 seconds of integration. The diamond marks the blue-peakup flux density.

observation of CFRS 14.1157, a faint galaxy at a redshift of z = 1.15 [25].

The results from the IRS observations by Higdon et al. [26] are summarised here. Figure 6 shows the IRS blue peak-up camera image, which is used to accurately determine the position of the source so that it can be placed on the IRS slits. This also gives an independent measure of the flux density at 16 μm. The peak up images revealed two serendipitous detections of the galaxies CFRS 14.9025 and CFRS 14.1129. The slit orientation fortuitously included CFRS 14.9025. This source has a flux of 0.35 mJy at 16 μm and the IRS-LL spectrum is shown in Figure 7.

Figure 8 shows the CFRS 14.1157 MIR spectrum, which is featureless apart from a broad absorption dip at $\sim$ 19 μm. The redshift is determined using a simple template fitting algorithm in which discrete emission and absorption features from template starburst and AGN spectra are redshifted over the interval $0 < z < 3$ in steps of 0.04, regridded, scaled, and then compared to the IRS source spectra. The feature at $\sim$ 19 μm is attributed to silicate absorption at a rest wavelength $\sim$ 9.7 μm corresponding to a redshift of 1.00 ± 0.20. This result is consistent with the optically

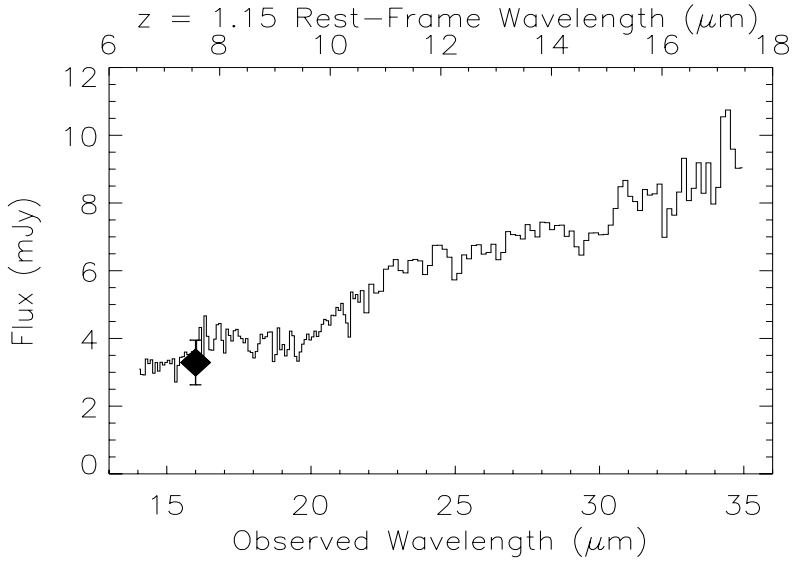

FIGURE 8. IRS-LL spectrum of CFRS 14.1157 (z = 1.15) obtained after 2880 seconds of integration. The diamond marks the blue-peakup flux density.

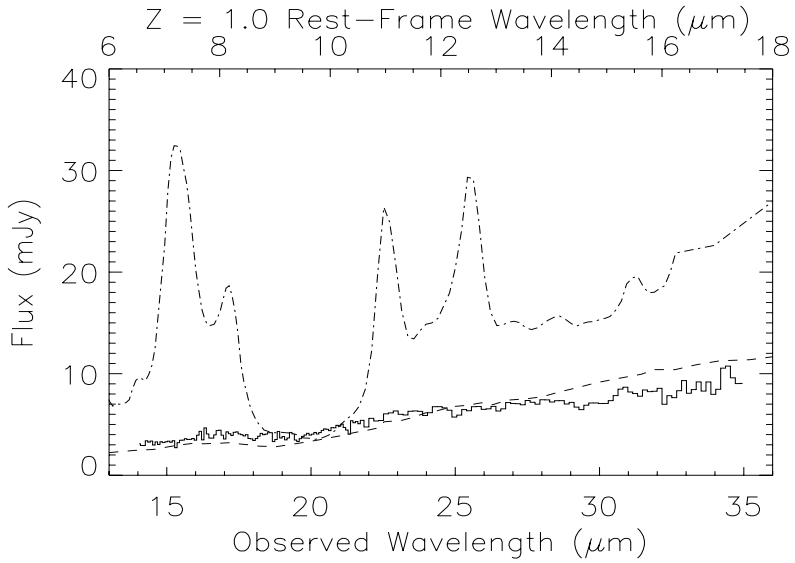

FIGURE 9. CFRS 14.1157 overlaid with the mid-infrared spectra of M82 (dot-dash line) and NGC 1068 (dash line) redshifted to z = 1.0, as determined by the MIR fit. The spectra of M 82 and NGC 1068 are from ISO-SWS [22]

determined redshift of 1.15 and gives us confidence that the silicate feature can be used to secure redshifts for galaxies too faint for optical spectroscopy.

As illustrated in Figure 9 there is no evidence for PAH emission. The 7.7 μm (11.3 μm) PAH emission relative to the continuum must be at least 24 (12) times fainter than observed in M82. In nearby galaxies the flux at 15 μm is strongly correlated with the infrared luminosity, with $L_{IR} \sim 11.1\, L_{15\mu m}$ [27]. If this correlation holds for more distant galaxies, then the IR luminosity of CFRS 14.1157 is $\sim 10^{13}\ L_{\odot}$, i.e., it is a hyper-luminous infrared galaxy. The lack of detectable PAH emission may not be surprising as there are indications in the local universe for sources with $L_{IR} \geq 10^{12.4}\ L_{\odot}$ to be dominated by emission from an AGN in the mid-infrared [28].

These observations have clearly demonstrated the ability of the IRS-LL to determine the redshift of faint galaxies ($F_{16\mu m}$ = 3.6 mJy). An rms of 0.3 mJy is reached after 2880 seconds of integration. In the following section we discuss our program to survey the NOAO Boötes field and determine the star formation history out to redshifts of $\sim$ 3. Fitting the silicate absorption feature may be the only means of measuring redshifts of highly embedded sources.

STAR FORMATION HISTORY: THE BOÖTES SURVEY

Determining the star formation density of the Universe beyond z$\sim$1 and the contribution made by AGN to the luminosity evolution of galaxies are two fundamental goals of observational cosmology. In collaboration with the NOAO Deep Wide Field Survey (NDWFS) team (Buell Januzzi, Arjun Dey & Michael Brown) and members of the MIPS Instrument team (Marcia Rieke & Emeric Le Floc'h) the IRS instrument team is surveying $\sim$ 8 deg^2 of the NDWFS region in Boötes at 24, 70 and 160 μm. The results from this survey are being cross-catalogued with the NDWFS $\sim$ 9.5 deg^2 optical survey (5 σ point-source sensitivities in B_w, R, and I = 26 AB magnitudes) to discover optically "invisible" galaxies at redshifts of $\sim$ 2 - 3.

The MIPS survey has proved highly successful, for example, we found over 58,000 sources in $\sim$8 deg^2 to the 0.3 mJy completeness limit at 24 μm. The positional uncertainties are typically $\leq$ 0.3 $''$. The survey and analysis techniques have been described by Papovich et al. [29]. In the previous section we demonstrated that the IRS-LL can obtain a spectrum of an $F_{24} \geq$ 0.75 mJy source in approximately one hour of integration time. There are 4273 sources brighter than 0.75 mJy at 24 μm. For the first round of IRS-LL follow-up observations we have selected 27 sources that are optically faint/invisible i.e. B_w, R, & I $>$ 26 AB mag.

We have also conducted a deep VLA 20cm survey 0.6 deg^2 of the Boötes field (F_{20cm} = 76 μJy, 5 σ). The results summarised here are from Higdon et al. [30]. Twelve percent of the 371 compact radio sources have no optical counterparts in the NDWFS catalog i.e., are optically "invisible". The majority are not detected by MIPS at 24 μm to a limiting flux of 0.3 mJy. Comparisons of their 20 cm and 24 μm fluxes (or upper limits) with a range of galaxy spectral energy distributions indicate that this population is dominated by AGN rather than starburst galaxies. We also compared our multi-wavelength data to a published Chandra X-Ray survey by Wang et al. [31]. Eight percent of the 168 Chandra X-ray sources are optically invisible, with none detected by MIPS at 24 μm. The infrared to X-ray flux ratio limits are consistent with a dominant AGN. We conclude that both these populations of optically invisible radio and X-ray sources are relatively dust-poor AGN at high redshift.

SPITZER/IRS OBSERVATIONS OF THE REDSHIFT 3.91 QUASAR APM 08279+5255

At a redshift z = 3.91 [32], the quasar APM 08279+5255 is the most luminous object known in the universe. However, as originally suggested by Irwin et al. [33] and subsequently confirmed by Ibata et al. [34] and Egami et al. [35], APM 08279+5255 is strongly gravitationally lensed, with a magnification of $\sim$ 100. The intrinsic bolometric luminosity is therefore 5 $\times$ 10^{13} $L_\odot$. The lensed quasar system is both dust- and gas-rich, with detections in the millimeter and submillimeter continuum [36] and in multiple CO emission lines [32, 37]. This makes it a prime candidate in which to search for PAH emission at high redshift. The lensing makes it bright enough for study by the SST. APM 08279+5255 was observed with the IRS to assess the nature of quasars at very large look-back times. The results from Soifer et al. [38] are summarised here.

Figure 10 shows the IRS spectrum of APM 08279+5255. The presence of substantial emission at rest wavelengths $>$ 2 μm argues for high dust temperatures (T_{dust} $>$ 1000 K), approaching the sublimation temperature of silicate grains [39]. The change in the continuum slope at a rest wavelength of 3 μm is consistent with the destruction of dust grains.

Broad Paα and Paβ recombination lines of hydrogen are detected at wavelengths of 9.235 and 6.315 μm. The 900 kms^{-1} linewidths are consistent with the lines arising in the broad line regions (BLR) in quasars. The ratio Paα/Paβ of 1.05 $\pm$ 0.2 is far from both the case B value of 2 and a simple high density quasar BLR model value of 1.8. This deviation is opposite in sense to the expected effect of reddening and requires further modelling.

The non-detection of the 3.3 and 6.2 μm PAH emission features is consistent with the trend found in nearby type 1 AGNs and quasars, which show weak or non-existent PAHs [28]. Also, it should be noted that differential magnification in the gravitational lens could hide a PAH emission feature. For example a region of hot dust emission located close to the caustics would be highly magnified in contrast to the extended PAH emission and could substantially reduce the equivalent width of any PAH features in the observed spectrum.

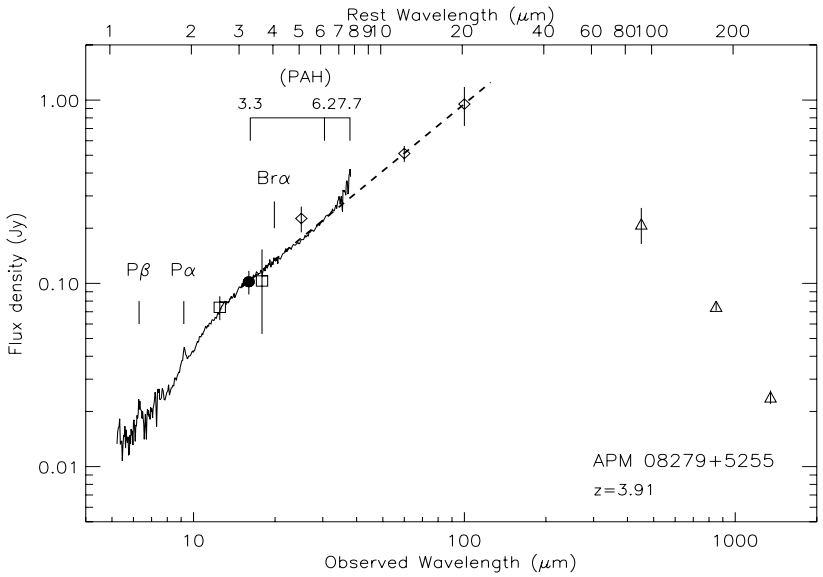

FIGURE 10. The smooth, steeply rising continuum is consistent with dust in an accretion disk heated by an underlying AGN. The continuum shows a steepening in the continuum for wavelengths < 15 μm (2.85 μm in the rest frame of the lensed quasar). This is suggestive of the temperature of sublimation of silicate grains in a quasar accretion disk.

SUMMARY

In the preceding Sections we have highlighted a few of the first results from the IRS Extragalactic Team. The wide area surveys by MIPS and IRAC are opening-up new discovery space and many of the results are already available in the public archive [2].

The unprecedented sensitivity of the IRS offers unique follow-up capabilities. SST has a limited and very precious lifetime and we urge all astronomers to consider how it can best be used to further our understanding of the Universe.

ACKNOWLEDGMENTS

I would like to thank Mr G. P. & Mrs C. W. Mitchell for sponsoring the symposium. I also thank Dr Roland Allen for inviting me to speak at the conference. The conference was excellent and my thanks to all those that helped make it a success. I look forward to the Second Mitchell Symposium.

We thank the IRS team and Spitzer Science Center for their continued dedication to the success of the SST mission.

This work is based (in part) on observations made with the Spitzer Space Telescope, which is operated by the Jet Propulsion Laboratory, California Institute of Technology under NASA contract 1407. Support for this work was provided by NASA through contract 1257184, issued by JPL/Caltech.

REFERENCES

1. Werner, M. W., L., R. T., Low, F. J., Rieke, M., G. H.and Rieke, Hoffmann, W. F., Young, E., Houck, J. R., Brandl, G. G., B.and Fazio, Hora, J. L., Gehrz, R. D., Helou, G., Soifer, B. T., Stauffer, J., Keene, J. K., Eisenhardt, P., Gallagher, D., Gautier, T. N., Irace, W., Lawrence, C. R., Simmons, L., Van Cleve, J. E., Jura, M., Wright, E. L., and Cruikshank, D. P., *ApJS*, **154**, 1 (2004).

[2] `http://ssc.spitzer.caltech.edu/archanaly/archive.html`

2. Houck, J. R., Roellig, T. L., van Cleve, J., Forrest, W. J., Herter, T., Lawrence, C. R., Matthews, K., Reitsema, H. J., Soifer, B. T., Watson, D., Weedman, D., Huisjen, M., Troeltzsch, J., Barry, D. J., Bernard-Salas, J., Blacken, C. E., Brandl, B. R., Charmandaris, V., Devost, D., Gull, G. E., Hall, P., Henderson, C. P., Higdon, S. J. U., Pirger, B. E., Schoenwald, J., Sloan, G. C., Uchida, . I., Appleton, P. N., Armus, L., Burgdorf, M. J., Fajardo-Acosta, S. B., Grillmair, C. J., Ingalls, J. G., Morris, P. W., and Teplitz, H. I., *ApJS*, **154**, 18 (2004).
3. Fazio, G. G., Hora, J. L., Allen, L. E., Ashby, M. L. N., Barmby, P., Deutsch, L. K., Huang, J.-S., Kleiner, S., Marengo, M., Megeath, S. T., Melnick, G. J., Pahre, M. A., Patten, B. M., Polizotti, J., Smith, H. A., Taylor, R. S., Wang, Z., Willner, S. P., Hoffmann, W. F., Pipher, J. L., Forrest, W. J., McMurty, C. W., McCreight, C. R., McKelvey, M. E., McMurray, R. E., Koch, D. G., Moseley, S. H., Arendt, R. G., Mentzell, J. E., C. T. Marx, P., Losch, ., Mayman, P., Eichhorn, W., Krebs, D., Jhabvala, M., Gezari, D. Y., Fixsen, D. J., Flores, J., Shakoorzadeh, K., Jungo, R., Hakun, C., Workman, L., Karpati, G., Kichak, R., Whitley, R., Mann, S., Tollestrup, E. V., Eisenhardt, P., Stern, D., Gorjian, V., Bhattacharya, B., Carey, S., Nelson, B. O., Glaccum, W. J., Lacy, M., Lowrance, P. J., Laine, S., Reach, W. T., Stauffer, J. A., Surace, J. A., Wilson, G., Wright, E. L., Hoffman, A., Domingo, G., and Cohen, M., *ApJS*, **154**, 10 (2004).
4. Rieke, G. H., Young, E. T., Engelbracht, C. W., Kelly, D. M., Low, F. J., Haller, E. E., Beeman, J. W., Gordon, K. D., Stansberry, J. A., Misselt, K. A., Cadien, J., Morrison, J. E., Rivlis, G., Latter, W. B., Noriega-Crespo, A., Padgett, D. L., Stapelfeldt, K. R., Hines, D. C., Egami, E., Muzerolle, J., Alonso-Herrero, A., Blaylock, M., Dole, H., Hinz, J. L., Floc'h, E. L., Papovich, C., Pérez-González, P. G., Smith, P. S., Su, K. Y. L., Bennett, L., Frayer, D. T., Henderson, D., Lu, N., Masci, F., Pesenson, M., Rebull, L., Rho, J., Keene, J., Stolovy, S., Wachter, S., Wheaton, W., Werner, M. W., and Richards, P. L., *ApJS*, **154**, 25 (2004).
5. Armus, L. H., M., T., and Miley, G. K., *AJ*, **94**, 831 (1987).
6. Sanders, D. B., Soifer, B. T., Elias, J. H., Madore, K., B. F.; Matthews, Neugebauer, G., and Scoville, N. Z., *ApJ*, **325**, 74 (1988).
7. Murphy, J., T. W., Armus, L., Matthews, K., Soifer, B. T., Mazzarella, J. M., Shupe, D. L., Strauss, M. A., and Neugebauer, G., *AJ*, **111**, 1025 (1996).
8. Mihos, C. J., and Hernquist, L., *ApJ*, **464**, 641 (1996).
9. Blain, A. W., Smail, I., Ivison, R. J., Kneib, J.-P., and Frayer, D. T., *Phys. Rev.*, **369**, 111 (2002).
10. Armus, L., Charmandaris, V., Spoon, H. W. W., Houck, J. R., Soifer, B. T., Brandl, B. R., Appleton, P. N., Teplitz, H. I., Higdon, S. J. U., Weedman, D. W., Devost, P. W., D.and Morris, Uchida, K. I., van Cleve, J., Barry, G. C., D. J.and Sloan, Grillmair, C., Burgdorf, M. J., Fajardo-Acosta, S. B., Ingalls, J. G., J. Higdon, J., Hao, L., Bernard-Salas, J., Herter, T., Troeltzsch, J., Unruh, B., and Winghart, M., *ApJS*, **154**, 178 (2004).
11. Veilleux, S., Kim, D. C., Sanders, J. M., D. B.and Mazzarella, and Soifer, B. T., *ApJS*, **98**, 171 (1995).
12. Genzel, R., Lutz, D., Sturm, E., Egami, E., Kunze, D., Moorwood, A. F. M., Rigopoulou, D., Spoon, H. W. W., Sternberg, A., Tacconi-Garman, L. E., Tacconi, L., and Thatte, N., *ApJ*, **498**, 589 (1998).
13. Imanishi, M., Terashima, Y., Anabuki, N., and Nakagawa, T., *ApJ*, **596**, L167 (2003).
14. Mazzarella, J. M., Gaume, R. A., Soifer, B. T., Graham, J. R., Neugebauer, G., and Matthews, K., *AJ*, **102**, 1241 (1991).
15. Shuder, J. M., and Osterbrock, D. E., *ApJ*, **250**, 55 (1981).
16. Miller, J. S., and Goodrich, R. W., *ApJ*, **355**, 456 (1990).
17. Goodrich, R. W., Veilleux, S., and Hill, G. J., *ApJ*, **422**, 521 (1994).
18. Veilleux, S., Goodrich, R. W., and Hill, G. J., *ApJ*, **477**, 631 (1997).
19. MacKenty, J. W., and Stockton, A., *ApJ*, **283**, 64 (1984).
20. Sanders, D. B., Soifer, B. T., Elias, J. H., Neugebauer, G., and Matthews, K., *ApJ*, **328**, L35 (1988).
21. Moutou, C., Verstraete, L., Leger, A., Sellgren, K., and Schmidt, W., *A&A*, **354**, L17 (2000).
22. Sturm, E., Lutz, D., Tran, D., Feuchtgruber, H., Genzel, R., Kunze, D., Moorwood, A. F. M., and Thornley, M. D., *A&A*, **358**, 481 (2000).
23. Smith, J. D. T., Dale, D. A., Armus, L., Draine, B. T., Hollenbach, D. J., Roussel, H., Helou, G., R. C. Kennicutt, J., Li, A., Bendo, G. J., Calzetti, D., Engelbracht, C. W., Gordon, K. D., Jarrett, T. H., Kewley, L., Leitherer, C., Malhotra, S., Meyer, M. J., Murphy, E. J., Regan, M. W., Rieke, G. H., Rieke, M. J., Thornley, M. D., Walter, F., and Smith, M. G. W., *ApJS*, **154**, 199 (2004).
24. Sturm, E., Lutz, D., Verma, A., Netzer, H., Sternberg, A., Moorwood, A. F. M., Oliva, E., and Genzel, R., *A&A*, **393**, 821 (2002).
25. Hammer, F., Crampton, D., Lilly, S., Le Fevre, O., and Kenet, T., *MNRAS*, **276**, 1085 (1995).
26. Higdon, S. J. U., Weedman, D., Higdon, J. L., Herter, T., Charmandaris, V., Houck, J. R., Soifer, B. T., Brandl, B. R., Armus, L., and Hao, L., *ApJS*, **154**, 174 (2004).
27. Chary, R., and Elbaz, D., *ApJ*, **556**, 562 (2001).
28. Tran, Q. D., Lutz, D., Genzel, R., Rigopoulou, D., Spoon, H. W. W., Sturm, E., Gerin, M., Hines, D. C., Moorwood, A. F. M., Sanders, D. B., Scoville, N., Taniguchi, Y., and Ward, M., *ApJ*, **552**, 527 (2001).
29. Papovich, C., Dole, H., Egami, E., Floc'h, L., Perez-Gonzalez, P., Gai, L., Beichman, C., Blaylock, M., Engelbracht, C., Gordon, K., Hines, D., Misselt, K., Morrison, J., Mould, J., Muzerolle, J., Neugebauer, G., Richards, P., Rieke, M., G.and Rieke, Rigby, J., Su, K., and Young, E., *ApJS*, **154**, 70 (2004).
30. Higdon, J. L., Higdon, S. J. U., Weedman, D. W., Houck, J. R., le Floc'h, E., Brown, M. J. I., Dey, A., Jannuzi, B. T., Soifer, B. T., and Rieke, M. J., *ApJ (submitted)* (2004).
31. Wang, J. X., Malhotra, S., Rhoads, J., Brown, M., Dey, A., Heckman, T., Jannuzi, B., Norman, C., Tiede, G., and Tozzi, P., *AJ*, **127**, 213 (2004).

32. Downes, D., Neri, R., Wiklind, T., Wilner, D. J., and Shaver, P. A., *ApJ*, **513**, L1 (1999).
33. Irwin, M. J., Ibata, R. A., Lewis, G. F., and Totten, E. J., *ApJ*, **505**, 529 (1998).
34. Ibata, R. A., Lewis, G. F., Irwin, M. J., Lehár, J., and Totten, E. J., *AJ*, **118**, 1922 (1999).
35. Egami, E., Neugebauer, G., Soifer, B. T., Matthews, K., Ressler, M., Becklin, E. E., Murphy, T. W., and Dale, D. A., *ApJ*, **535**, 561 (2000).
36. Lewis, G. F., Chapman, S. C., Ibata, R. A., Irwin, M. J., and Totten, E. J., *ApJ*, **505**, L1 (1998).
37. Papadopoulos, P., Ivison, R., Carilli, C., and Lewis, G., *Nat.*, **409**, 58 (2001).
38. Soifer, B., Charmandaris, V., Brandl, B. R., Armus, L., Appleton, P. N., Burgdorf, M. J., Devost, D., Herter, T., Higdon, S. J. U., Higdon, J. L., Houck, J. R., Lawrence, C. R., Morris, P. W., Teplitz, H. I., Uchida, K. I., van Cleve, J., and Weedman, D., *ApJS*, **154**, 151 (2004).
39. Salpeter, E. E., *ApJ*, **193**, 579 (1974).